PERGAMON

Current Opinion in Solid State and Materials Science 4 (1999) 141–153

Current Opinion in **Solid State & Materials Science**

From giant molecular clusters and precursors to solid-state structures

A. Müller[a,*], D. Fenske[b,*], P. Kögerler[a]

[a]*Fakultät für Chemie, Universität Bielefeld, Postfach 100131, 33501 Bielefeld, Germany*
[b]*Institut für Anorganische Chemie 1, Universität Karlsruhe, Engesserstraße, Geb. 30.45, 76128 Karlsruhe, Germany*

Abstract

Novel nanosized ring-shaped polyoxometalate and ligand-protected metal chalcogenide clusters provide versatile models for the study of molecular growth processes, especially at the interface to solid-state chemistry. Besides their unusual electronic properties, their use as synthons or precursors for solid-state structures with tailored properties, such as mesoporosity, raises special interest for materials science (polyoxometalate case).

1. Introduction

One of the most challenging problems in contemporary chemistry is the deliberate and especially synthon-based synthesis of multifunctional compounds and materials—including those with network structures—with desirable or predictable properties, such as mesoporosity (well-defined cavities and channels), electronic and ionic transport, ferro- as well as ferrielasticity, luminescence, and catalytical activity. Transition metal chalcogen compounds are of special interest in that respect. To give an example, the deeply coloured, mixed-valence transition metal-oxides—especially the so-called hydrogen molybdenum bronzes—with their unusual property of high conductivity and wide range of composition play an important role in technology, industrial chemical processes, and materials science [1–3]. Their field of application ranges from electrochemical elements, hydrogenation and dehydrogenation catalysts, super-conductors, passive electrochromic display devices, to 'smart' windows. The synthesis of such compounds or solids from preorganized linkable building blocks (synthons) with well-defined geometries and well-defined

*Corresponding authors. Tel.: +49-521-1066-153; fax: +49-521-1066-003.

E-mail address: a.mueller@uni-bielefeld.de (A. Müller)

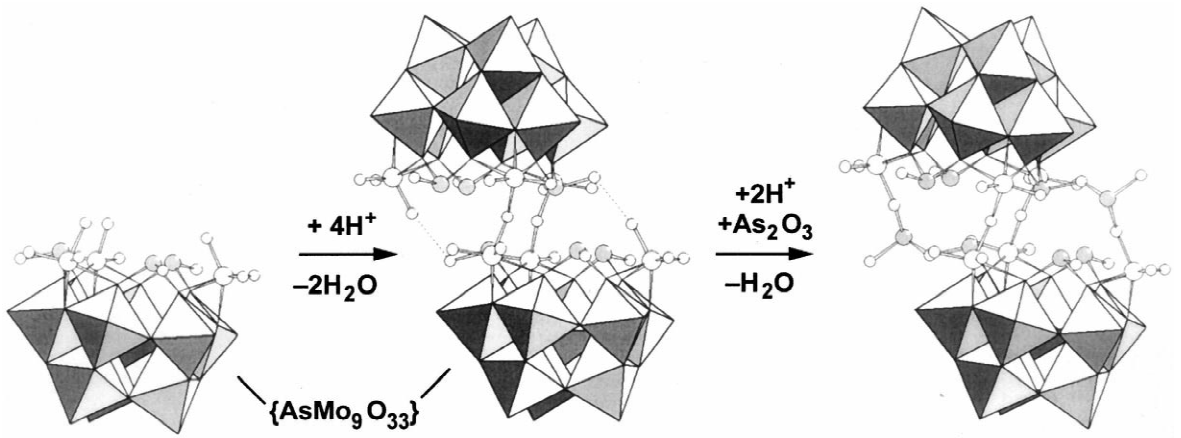

Fig. 1. Condensation reactions to $[(AsOH)_6(MoO_3)_2(O_2MoOMoO_2)_2(AsMo_9O_{33})_2]^{10-}$ (middle) and $[(AsOH)_4(AsO)_2(HOAsOMoO_2)_2(O_2MoOMoO_2)_2-(AsMo_9O_{33})_2]^{8-}$ (right) based on the functionalization of $\{AsMo_9O_{33}\}$ fragments (polyhedral representation) with three highly reactive facial $\{MoO_3\}$ groups in $[(AsOH)_3(MoO_3)_3(AsMo_9O_{33})]^{7-}$ (left) are possible.

1359-0286/99/$ – see front matter
PII: S1359-0286(99)00015-7

Nomenclature

Me	methyl, CH_3
Et	ethyl, C_2H_5
Ph	phenyl, C_6H_5
^{n}Bu	*n*-butyl, C_4H_9
^{t}Bu	*tert*-butyl, C_4H_9
Mes	mesityl, C_7H_7
^{n}Pr	*n*-propyl, C_3H_7

chemical properties is therefore of special interest to this end [4]. In this short review, we will focus on this substance class and on coin metal-based chalcogenide clusters, stressing in the present case the evident relation between giant clusters and typical solid-state structures.

2. Giant clusters as synthons (precursors) for solid-state structures

2.1. Basic principles and examples for the synthesis of ever larger molybdenum oxide-based giant clusters: synthons for network structures

In generating large complex molecular systems we have to realize that natural processes are effected by the (directed as well as non-directed) linking of a huge variety of basic and well-defined fragments. An impressive example of this, discussed in virtually all textbooks on biochemistry, is the self-aggregation process of the tobacco mosaic virus, which is based on preorganized units [5]. This process more or less meets our strategy in controlling the linking of fragments to form larger units and linking the latter again.

In the case of metal-oxide based clusters this means for instance that relatively large molecular fragments can

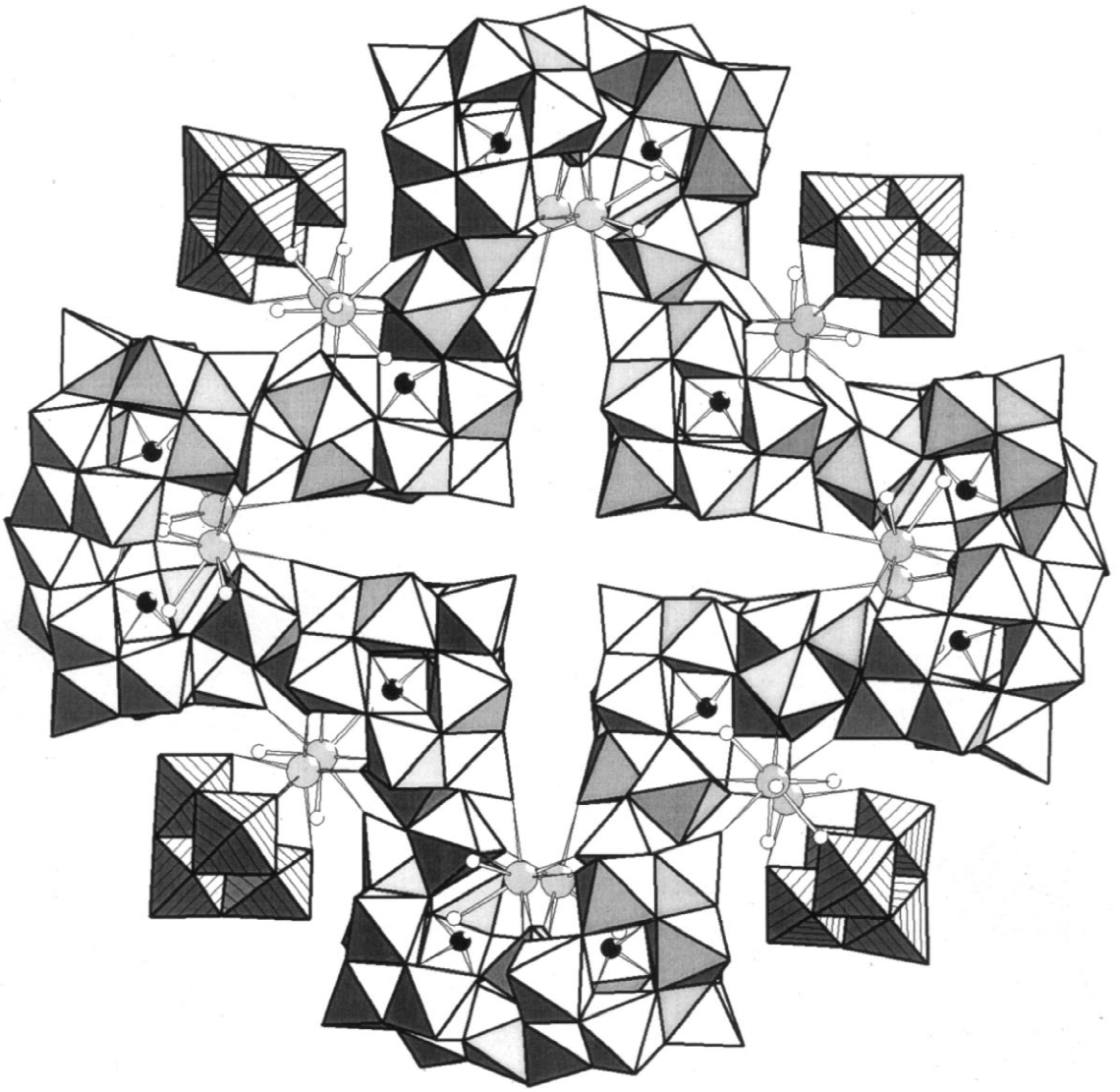

Fig. 2. Structure of the anion $[Ln_{16}As_{12}W_{148}O_{524}(H_2O)_{36}]^{76-}$ as a folded cyclic assembly of 12 lacunary $\{AsW_9\}$ groups linked by additional tungsten centers and four $\{LnW_5\}$ groups.

principally be functionalized with groups which allow linking through characteristic reactions: the protonation of highly reactive 'anti-Lipscomb' $\{MoO_3\}$ groups positioned on polyoxometalate cluster fragments for example, results in condensation reactions of the fragment under H_2O formation (Fig. 1) [6]. The same principle basically applies also for lacunary polyoxotungstates that can be linked by transition metal and lanthanide ions to form several large heteropolytungstate anions such as $[Ce_4(H_2O)_{4-4x}(AsW_9O_{33})_4As(WO_3)_{2+x}(WO_5)]^{25-}$ ($x < 0.5$) [7] or $[Ce_{16}As_{12}W_{148}O_{524}(H_2O)_{36}]^{76-}$ [8] (Fig. 2).

In our actual case, i.e. the generation of large polyoxometalate clusters [9,10], the above-mentioned concept of preorganized units is of particular importance due to the fact that the structural chemistry here is governed by *differently transferable building units*. As an archetypical example, the linking of polyoxometalate building blocks containing 17 molybdenum atoms ($\{Mo_{17}\}$ units) can

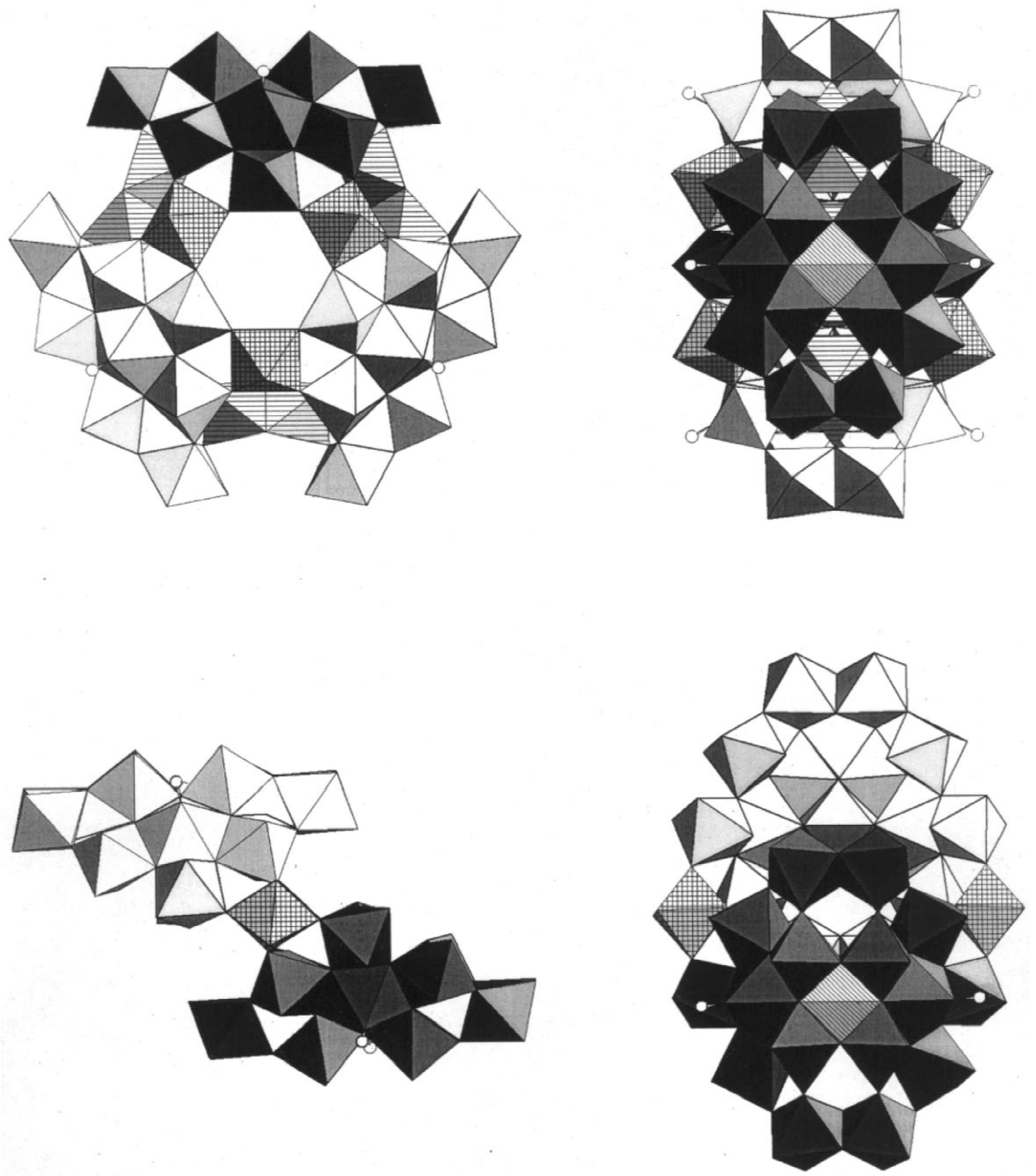

Fig. 3. Polyhedral representation of the $\{Mo_{57}\}$-type cluster with its building blocks along the C_3 (upper left) and one of the three C_2 axes (upper right): on the upper right, one $\{Mo_{17}\}$ group consisting of one $\{Mo_1'\}$ and two $\{Mo_8\}$ groups and on the upper left, one $\{Mo_8\}$ unit is highlighted. For comparison polyhedral representations of the $\{Mo_{36}\}$ cluster structure, consisting of two $\{Mo_{17}\}$ groups linked by two $\{Mo_1^*\}$ units, are shown in the related views, also highlighting one $\{Mo_8\}$ (bottom left) and one $\{Mo_{17}\}$ unit (bottom right). The $\{Mo_8\}$ group consists of a central pentagonal MoO_7 bipyramid to which five MoO_6 octahedra are linked sharing edges and two peripheral MoO_6 octahedra sharing corners with former octahedra.

be given, which results in the formation of cluster anions consisting of two or three of these units. The resulting species are of the $\{Mo_{36}\}$ (e.g. $[(MoO_2)_2\{H_{12}Mo_{17}(NO)_2O_{58}(H_2O)_2\}_2]^{12-}$, a two-fragment cluster) or of the $\{Mo_{57}\}$ type (e.g. $[(VO(H_2O))_6(Mo_2(H_2O)_2(OH))_3\{Mo_{17}(NO)_2O_{58}(H_2O)_2\}_3]^{21-}$, a three-fragment cluster) [11–13], the latter of which can be obtained from the former cluster under reducing conditions in the presence of the relatively strong nucleophilic linker V^{IV}. Furthermore, the structure of the $\{Mo_{17}\}$ unit can formally be reduced to smaller constituents: two $\{Mo_8\}$-type groups linked by $\{Mo_1'\}$-type units. The $\{Mo_8\}$ building block is found in many other large polyoxometalate structures and can again be divided into a (close packed) $\{(Mo)Mo_5\}$ pentagon built up by a central MoO_7 pentagonal bipyramid sharing edges with five MoO_6 octahedra and two more loosely bound MoO_6 octahedra sharing 'only' corners with atoms of the pentagon (Fig. 3). This implies that a remarkable superfullerene-type chemistry based on the pentagons is possible [14].

In solutions containing these clusters the (more reduced) giant mixed-valence wheel-shaped cluster $\{Mo_{154}\}$ $\{[Mo_{154}(NO)_{14}O_{434}(OH)_{14}(H_2O)_{70}]^{28-}\}$ forms upon reduction and further acidification [15]. This cluster can be regarded as a tetradecamer with D_{7d} symmetry (if the hydrogen atoms are excluded). It can be formally generated by linking 140 MoO_6 octahedra and 14 $MoO_6(NO)$ pentagonal square-pyramids (Fig. 4). The building

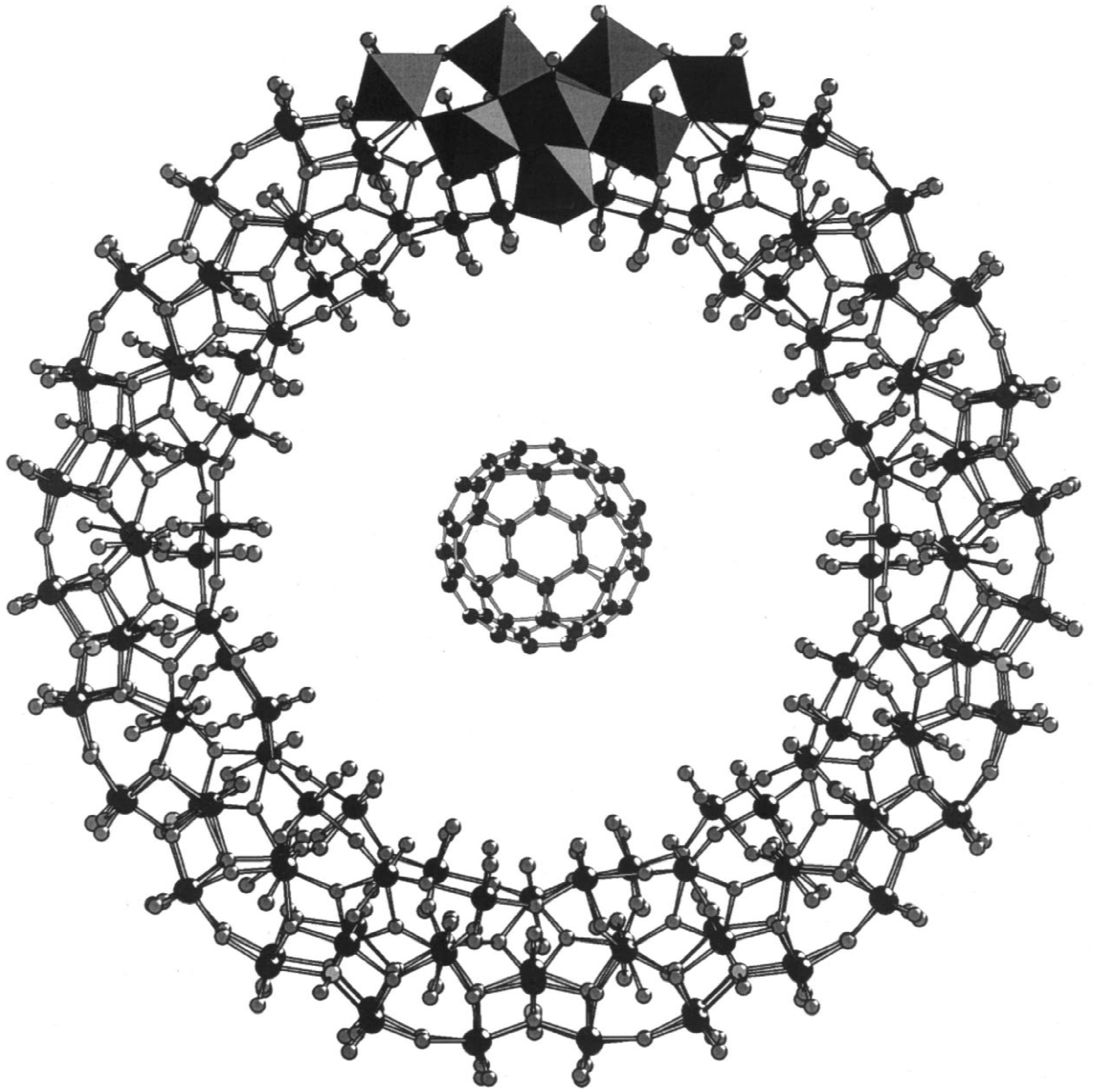

Fig. 4. Ball-and-stick representation of the cluster anion $\{Mo_{154}\}$ with one $\{Mo_8\}$ unit in polyhedral representation. For the purpose of size comparison a C_{60} fullerene molecule is shown.

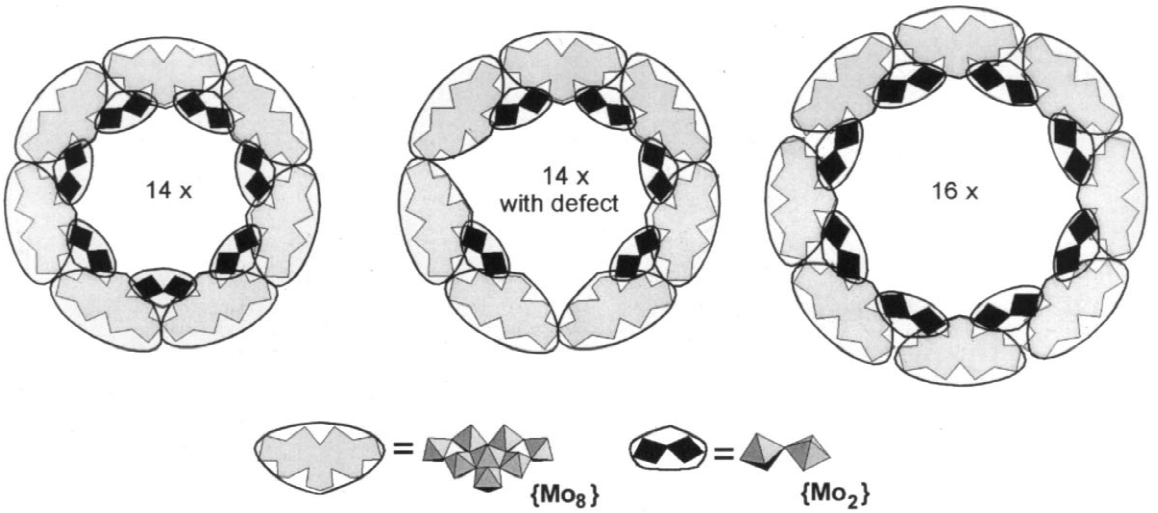

Fig. 5. Schematic comparison of the $\{Mo_{154}\}$ and $\{Mo_{176}\}$ cluster types showing the $\{Mo_8\}$ and $\{Mo_2\}$ units (the equatorial $\{Mo_1\}$ units are not visible in this representation).

blocks of the type $\{Mo_8\}$, $\{Mo_2\}$ and $\{Mo_1\}$ are each present 14 times not only in that cluster but also in the correspondingly 'pure' isopolyoxometalate cluster $[Mo_{154}O_{448}(OH)_{14}(H_2O)_{70}]^{14-}$ (having 14 $\{MoO\}^{4+}$ instead of 14 $\{MoNO\}^{3+}$ groups) which turned out to comprise one prototype of the soluble amorphous molybdenum blue species [16]. By formally adding two of each of the three different types of building units, the ring can even be expanded to the $\{Mo_{176}\}$ cluster with D_{8h} symmetry [17]. This presents a hexadecameric ring structure, containing correspondingly 16 instead of 14 of each of the three mentioned building blocks (Fig. 5). The important message is: a type of Aufbau principle seems to be valid for such cluster types. Interestingly their surfaces can even be modified by ligand-exchange reactions [18].

2.2. Crystal engineering: assembly of giant ring-shaped synthons to network structures via the synergetically induced complementarity of their surfaces

In the case of the $\{Mo_{154}\}$-type cluster, the nucleophilicity at special sites can be increased by either removing several positively charged $\{Mo_2\}^{2+}$ groups with bidentate ligands like formate (that means via formation of defects) [19] or by placing electron donating ligands like $H_2PO_2^-$ on the inner ring surfaces [20] (Figs. 6 and 7). This leads to a linkage of the ring-shaped clusters via Mo–O–Mo bonds to form compounds with layers or chains (derived from $\{Mo_{144}\}$ ring units [21]) (Fig. 8) according to a type of crystal engineering (see below). Single crystals of the chain-type compound exhibit interesting anisotropic electronic properties which represent promising fields for further research. In compounds of the former type channels are present, the inner surfaces of which have basic properties in contrast to the acidic channels in zeolites [22]. The layer compound can take up small organic molecules such as formic acid, which according to the basicity are partly deprotonated.

The reduction of an aqueous solution of sodium molybdate by hypophosphorous (phosphinic) acid at low pH

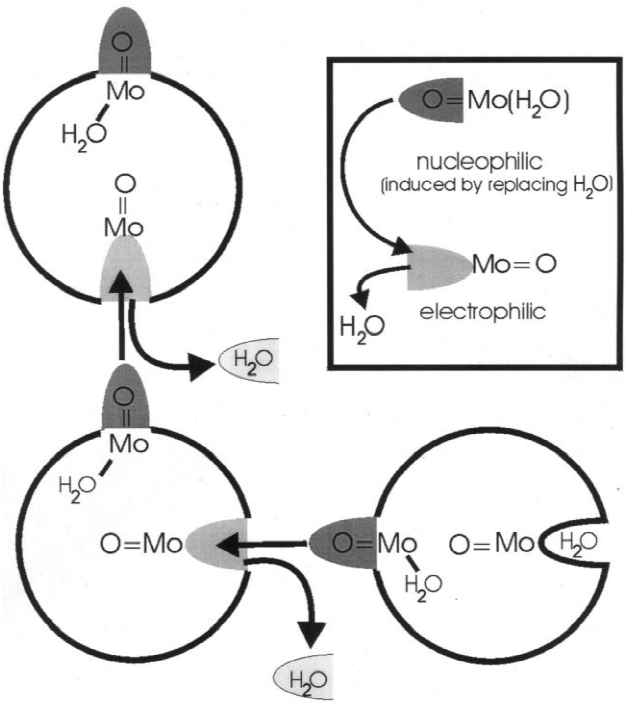

Fig. 6. Schematic representation of the synergetically induced assembly of ring-shaped cluster units to form a segment of a layer which is based on the induced functional complementarity of their surfaces: each ring contains functional complementary nucleophilic (due to the neighbouring electron donating ligands replacing H_2O) and electrophilic (after release of a H_2O ligand) groups.

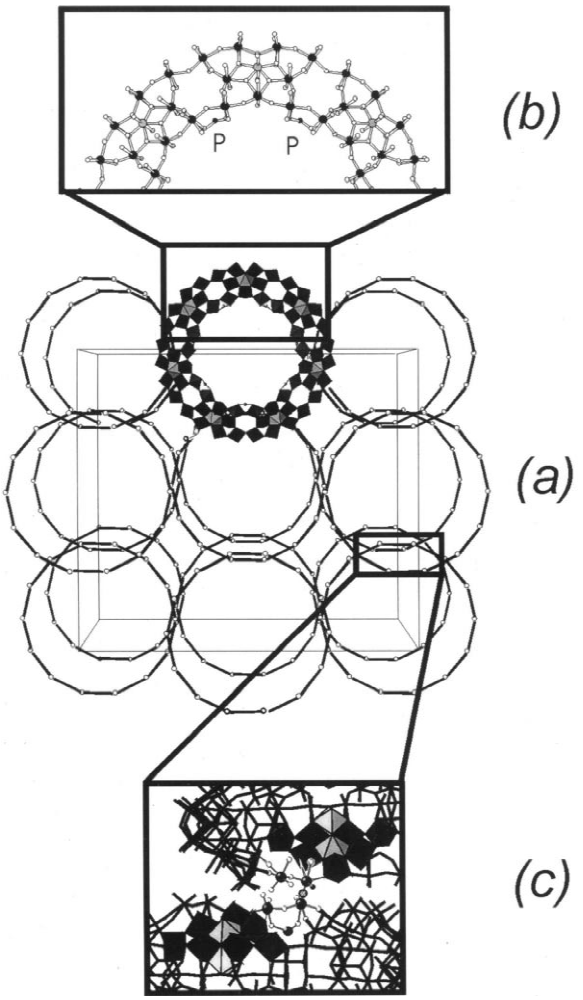

Fig. 7. (a) Perspective view of the framework (built up by linking the $[Mo_{154}O_{462}H_{14}(H_2O)_{54}(H_2PO_2)_7]$ cluster rings) along the crystallographic *c* axis, showing the abundance of nanotubes and cavities. For clarity, only one complete ring (without the P ligands) is shown in polyhedral representation. With respect to the other rings, only the centers of the $\{Mo_1\}$ units are given and connected. (b) Ball-and-stick representation of the upper half of a ring segment showing the position of the $H_2PO_2^-$ ligand. (c) Detailed view of the bridging region between two cluster rings emphasizing one $\{Mo_8\}$, one $\{Mo_1\}$ unit (in polyhedral representation) as well as one $\{Mo_2\}^{2+}$ unit and one $H_2PO_2^-$ ligand (in ball-and-stick representation). The bridging (disordered) oxygen center is depicted as a circle (see Ref. [19]).

values (≈1) results in the formation of nanosized ring-shaped cluster units which assemble to form layers of the compound $Na_{21}[Mo_{154}O_{462}H_{14}(H_2O)_{54}(H_2PO_2)_7]\cdot$ca. $300H_2O$ [20]. The assemblage is based on the synergetically induced complementarity of amphiphilic $\{Mo_2\}$-type $O{=}Mo(H_2O)$ groups and corresponds to the replacement of H_2O ligands of rings by related terminal oxo groups of the $\{Mo_2\}$-type O=Mo(L) units of other rings acting formally as ligands (and vice versa). The increased nucleophilicity of the O=Mo group at the ring is induced by coordinated $H_2PO_2^-$ ligands (Fig. 7).

2.3. A cluster as a guest in a cluster: an unusual supramolecular compound

Furthermore, $\{Mo_{148}\}$ defect clusters linked to chains can also act as hosts for smaller polyoxometalate clusters, such as the $\{Mo_{36}\}$-type cluster (Fig. 9). In this supramolecular system the interaction between host and guest, which fits exactly into the cavity of the host, is due to 16 hydrogen bonds as well as the Coulomb attraction mediated by four Na^+ cations located between the negatively charged host and guest [23].

3. A model for a nucleation and a limited growth process: sections of solid-state structures inside the cavities of molecular clusters

In describing or analyzing a solid-state structure, the following basic strategy is used: one decomposes, at least mentally, the given objects into elementary building blocks (e.g. polygons, polyhedra or aggregates of these) and then tries to identify and explore the local matching rules according to which the building blocks are to be assembled to yield the considered objects. A realistic model system for this procedure is given below. A new type of growth (nucleation) process within the cavity of the above-mentioned molecular $\{Mo_{176}\}$ cluster (which acts here as a compartment) has been observed, resulting in a $\{Mo_{248}\}$-type cluster [24] (see also Ref. [25]). This $\{Mo_{248}\}$ cluster basically consists of a $\{Mo_{176}\}$-type cluster ring, where the ring openings are covered by two {36Mo} ($=\{Mo_{36}(H_2O)_{24}O_{96}\}$) fragments which can be assigned to two hubcaps (these should not be confused with the $[Mo_{36}O_{112}(H_2O)_{16}]^{8-}$ ($\{Mo_{36}\}$) cluster) (Fig. 10). Important in context with the problem of understanding nucleation processes is (1) that the subunits within the hubcaps are similar (some are even identical) to those in the $\{Mo_{176}\}$-type cluster and (2) that these {36Mo} fragments represent (according to the first view) sections of the typical solid-state structure Mo_5O_{14}. The comparison of relevant parts of the $\{Mo_{248}\}$ cluster and the solid-state structure Mo_5O_{14} [26] reveals surprising parallels (Fig. 11): the hubcaps (if the H atoms of the H_2O ligands are excluded) are very similar to a section of the crystal lattice of Mo_5O_{14} (see Fig. 11). Important in this context is that detailed pathways for the initial growth (nucleation) steps of inorganic solid-state structures could not be recognized until now.

4. Clusters as sections of solid-state structures

The synthesis, structure, and physical properties of large metal clusters are currently being investigated in several research groups mainly to get ever larger clusters and study the quantum-size effect [27–36]. A part of this

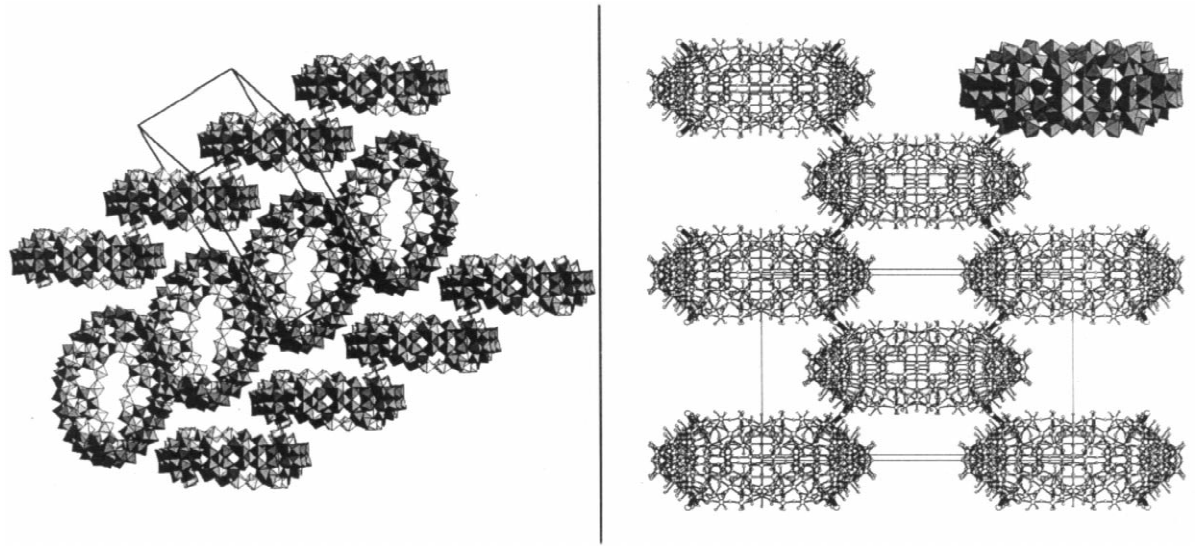

Fig. 8. Representation of parts of a chain-type structure ({Mo_{144}}, left) and a layer-type structure ({Mo_{152}}, right) both built up by linked ring-shaped units with defects.

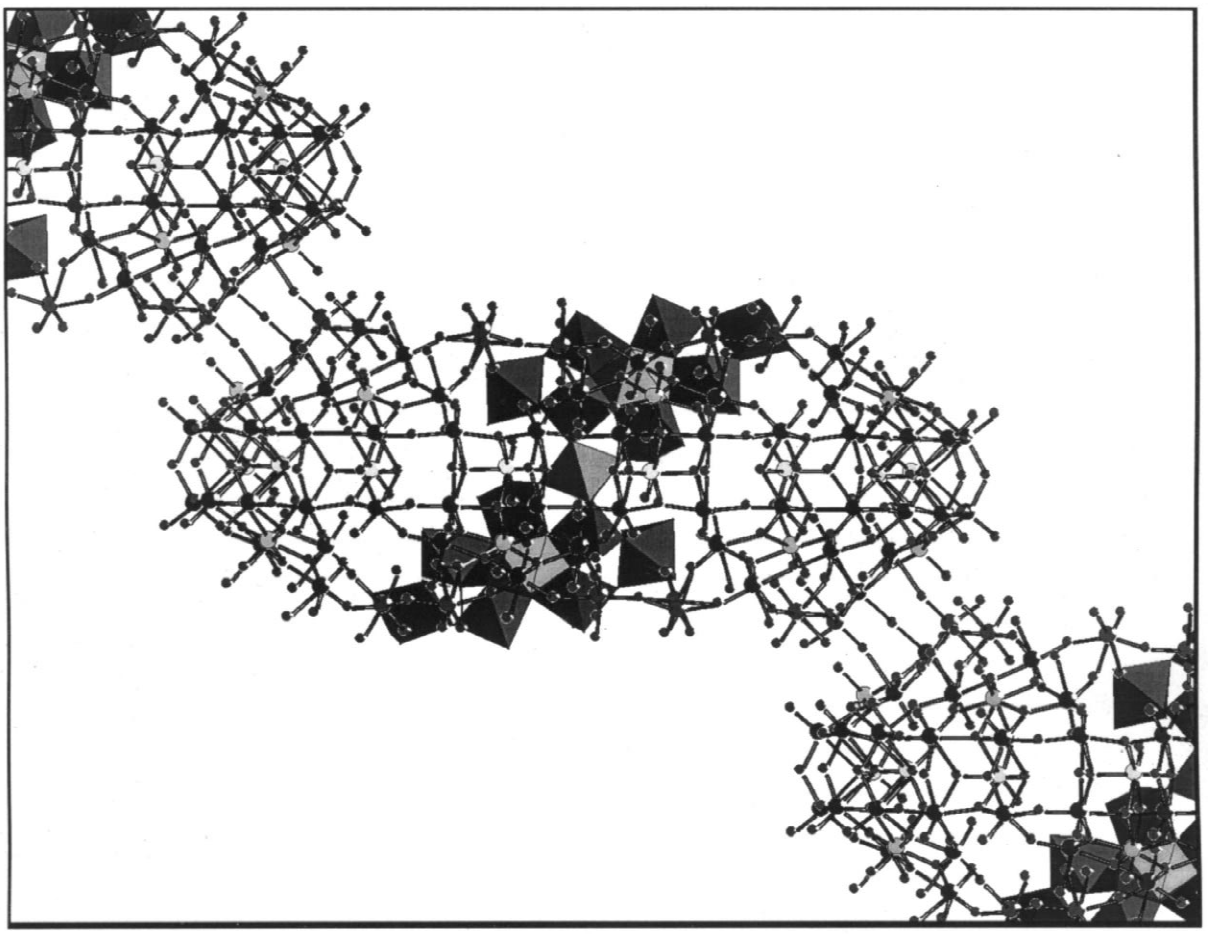

Fig. 9. Some structural details of the novel supramolecular system {$Mo_{36}\subset Mo_{148}$} ({Mo_{36}} occupation: ca. 20%). Part of the related chain structure is shown, which is built up by linking the ring-shaped clusters {Mo_{148}} which have three missing {Mo_2} groups. The interaction between host (in ball-and-stick representation) and guest (polyhedral representation) is due to 16 hydrogen bonds and four sodium cations localized between host and guest.

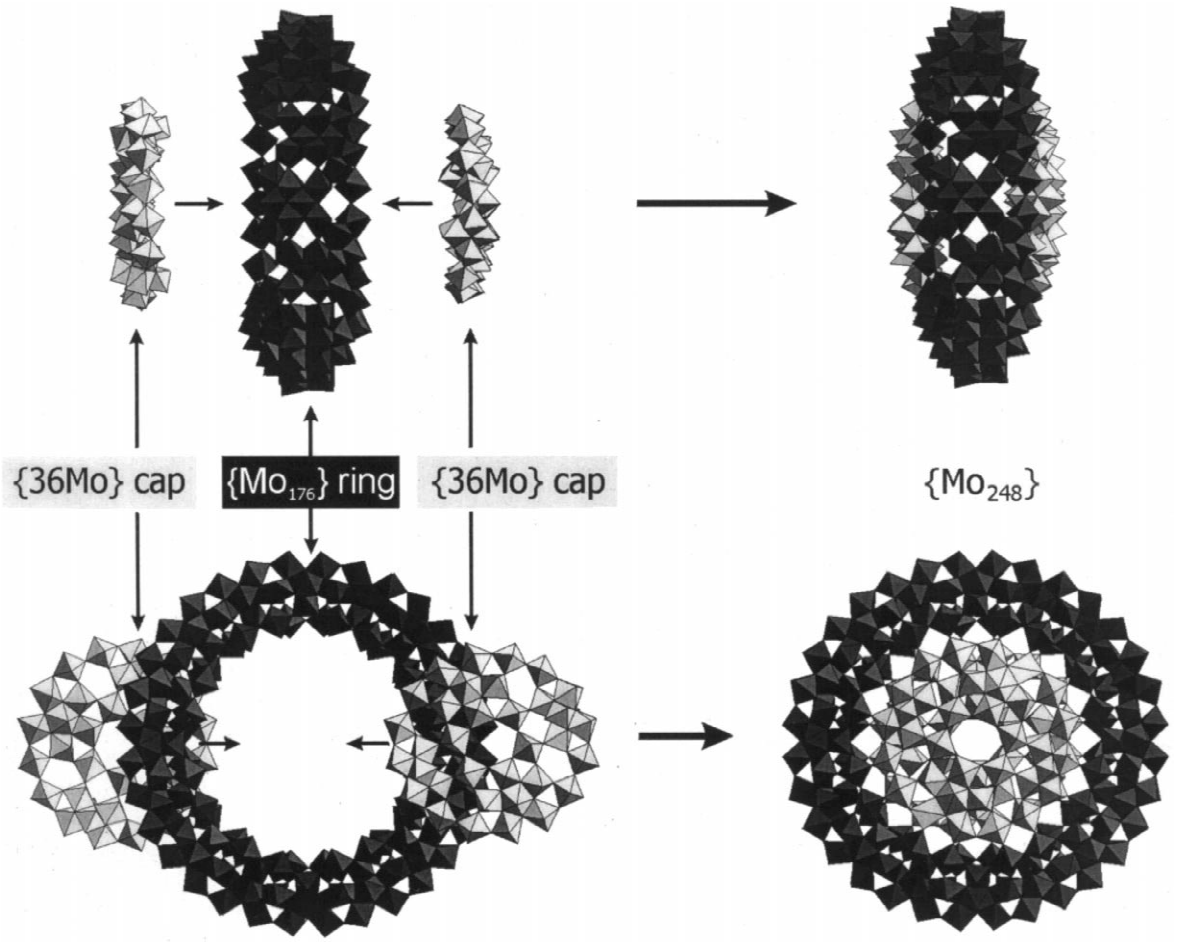

Fig. 10. Growth process of the type $\{Mo_{176}\}\rightarrow\{Mo_{248}\}$. The $\{Mo_{248}\}$-type cluster can formally be decomposed into two {36Mo} fragments and a $\{Mo_{176}\}$-type ring (above: side view, below: top view).

interest refers to the metal chalcogenide clusters. During the last few years interest in this class of compounds has increased dramatically, as they can be used as precursors in the production of semiconducting metal selenides and tellurides. A considerable number of multinuclear metal selenide cluster complexes are known now which are protected by a ligand shell avoiding further reaction to stable binary selenides. Examples are $[Ni_{34}Se_{22}(PPh_3)_{10}]$, $[Cu_{70}Se_{35}(PEt_3)_{22}]$, and $[Cu_{146}Se_{73}(PPh_3)_{30}]$ [37–40]. These compounds are formed by the reaction of PR_3 complexes (R=organic group) with metal halides and $Se(SiMe_3)_2$:

$$\mathrm{CuX} + \mathrm{PR_2R'} \xrightarrow[-\mathrm{SiMe_3X}]{\text{1. org. solvent}\ \text{2. } +\mathrm{E(SiMe_3)_2}} [\mathrm{Cu_{2n}E_n(PR_2R')_m}] \qquad \begin{array}{l}\mathrm{X = Cl, OAc}\\ \mathrm{R,R' = org.\ group}\\ \mathrm{E = S, Se}\end{array}$$

The mechanism for cluster formation and thus the molecular structure of the products, is strongly influenced by the special reaction conditions (temperature, type of copper salt used, type and size of the PR_3 ligand).

As expected very often the thermodynamically stable metal chalcogenides are formed, nonetheless, calculations have shown that the PR_3-stabilized cluster complexes are metastable [41–43]. Important in context with the aim of this review is that it is possible to obtain copper chalcogenide clusters which can be approximately described as a section of the structure of the binary Cu_2E phase (E=S, Se, Te) surrounded by PR_3 ligands. Though spherical cluster cores with up to 62 copper atoms do not permit a direct comparison with the binary copper chalcogenides, with increasing cluster size, one observes a 'transition' towards a layered Cu_2E-type skeleton. Fragments of the structure of the binary Cu_2Se phase can be recognized for the clusters $[Cu_{70}Se_{35}(PEt_3)_{22}]$ and $[Cu_{146}Se_{73}(PPh_3)_{30}]$ (Fig. 12). In particular, the relation to the Cu_2Se structure can be nicely seen by looking at the Se sublattices of the two cluster compounds. In both clusters there is a layered segment formed by the Se ligands, consisting of layers with 10, 15 and 10 Se ($\{Cu_{70}\}$) and 21, 31 and 21 Se atoms ($\{Cu_{146}\}$ cluster), respectively (Fig. 13). Most of the Cu atoms are positioned in the tetrahedral surroundings spanned by the Se atoms.

Whereas the reaction of AgCl for example with $Se(SiMe_3)_2$ in the presence of PR_3 usually affords insoluble

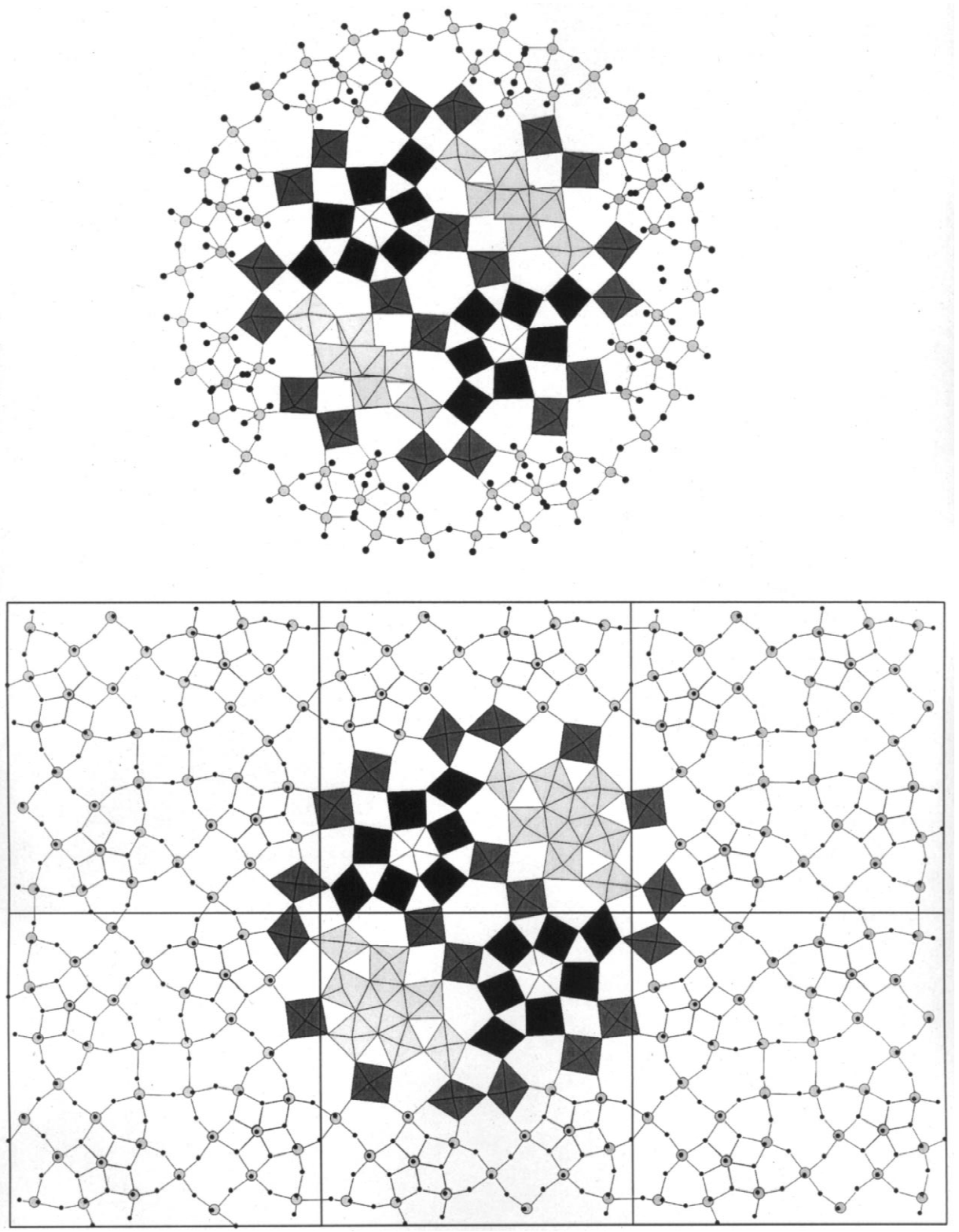

Fig. 11. Structural comparison of the hubcap motif of the $\{Mo_{248}\}$ cluster and the related segment of the solid-state structure Mo_5O_{14}. Above: schematic representation of one half of the $\{Mo_{248}\}$ cluster with a highlighted $\{36Mo\}$ hubcap. Below: structure of Mo_5O_{14} viewed along the *c* axis. Both the hubcaps and the Mo_5O_{14} layer sections each contain four $\{Mo_8\}$ entities surrounding two central $\{Mo_2\}$ units. A central ring of six MoO_6 octahedra is formed by these two $\{Mo_2\}$ units and two MoO_6 octahedra of two opposite $\{Mo_8\}$ entities. Whereas in the case of the Mo_5O_{14} 'layer' section all $\{Mo_8\}$ entities are of the type described above with one $\{(Mo)Mo_5\}$ pentagon which has two adjacent MoO_6 octahedra, in the case of the $\{Mo_{248}\}$ hubcaps two consist of a $\{Mo_6\}$ octahedron with two *trans*-positioned edge-sharing MoO_6 octahedra ($\{Mo_8'\}$ entities).

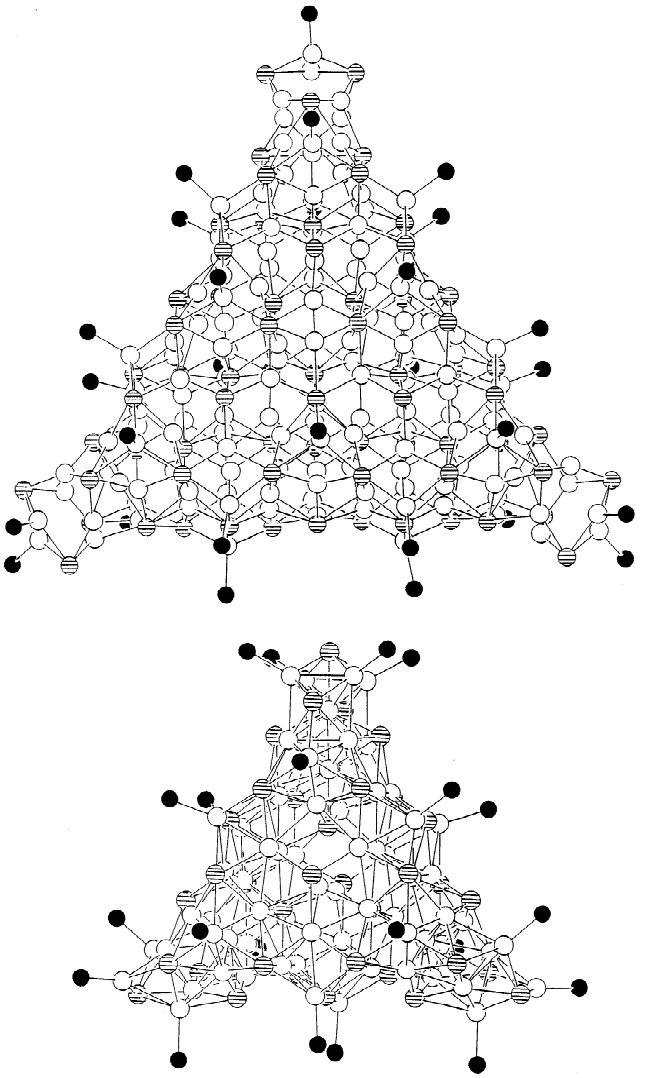

Fig. 12. Structure of $[Cu_{70}Se_{35}(PEt_3)_{22}]$ and $[Cu_{146}Se_{73}(PPh_3)_{30}]$ (without Et and Ph groups). ○, Cu; ◍, Se; ●, P.

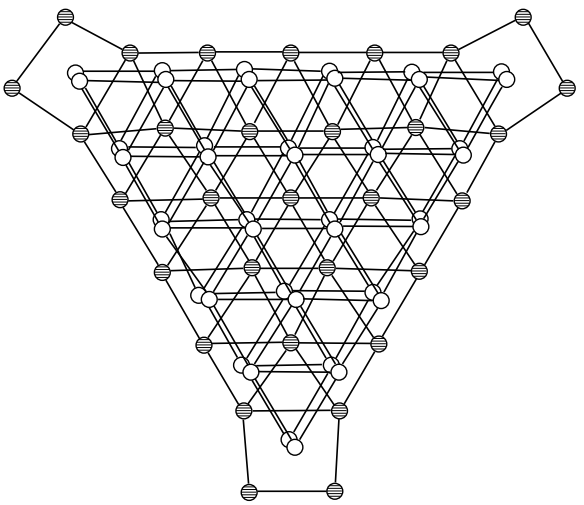

Fig. 13. Structure of the Se network in $[Cu_{146}Se_{73}(PPh_3)_{30}]$. ○, Se atoms of the first and third layers; ◍, Se atoms of the middle layer.

Ag_2Se, the corresponding reaction with $R'TeSiMe_3$ preferably provides silver clusters with Te^{2-} and TeR^- ligands. The structures of the compounds formed depend very much upon the type of the tertiary phosphane used and also on the organic group R′. Examples of related compounds with known structures are: $[Ag_6(\mu_3\text{-}Te^nBu)_4(\mu\text{-}Te^nBu)_2(PEt_3)_4]$, $[Ag_{10}(TePh)_{10}(PMe_3)_2]_\infty$, $[Ag_{30}(TePh)_{12}Te_9(PEt_3)_{12}]$, $[Ag_{32}(\mu_3\text{-}Te^nBu)_{18}Te_7(PEt_3)_6]$, $[Ag_{46}(TeMes)_{12}Te_{17}(PEt_3)_{16}]$, and $[Ag_{48}(\mu_3\text{-}Te^nBu)_{24}Te_{12}(PEt_3)_{14}]$ [44–46]. Other Ag clusters can be isolated from the reaction of silver carboxylates with $RSeSiMe_3$ and PR_3 or bidentate phosphanes. The reaction of P^nPr_3 with ^{t}BuSeSiMe$_3$ and silver benzoate in pentane at −40°C affords $[Ag_{30}Se_8(Se^tBu)_{14}(P^nPr_3)_8]$. Using the same reaction conditions with PEt_3 as ligands, only the formation of $[Ag_{90}Se_{38}(Se^tBu)_{14}(PEt_3)_{22}]$ can be observed [47].

$$[Ag_{90}Se_{38}(Se^tBu)_{14}(PEt_3)_{22}] \xleftarrow[PEt_3]{^t\text{BuSeSiMe}_3} Ag(C_6H_5CO_2)$$

$$\xrightarrow[P^nPr_3]{^t\text{BuSeSiMe}_3} [Ag_{30}Se_8(Se^tBu)_{14}(P^nPr_3)_8]$$

Interestingly, the $\{Ag_{90}\}$ cluster (Fig. 14) shows no similarity with the corresponding binary phase Ag_2Se but exciting structural details: the Se atoms form a torus-shaped polyhedron, which is built up from Se_3 faces (Fig. 15). The reaction of $Ag(C_{11}H_{23}CO_2)$ with ^{n}BuSeSiMe$_3$ and P^tBu_3 yields $[Ag_{114}Se_{34}(Se^nBu)_{46}(P^tBu_3)_{14}]$ (Fig. 16). If the monodentate phosphane ligands are replaced by bis(diphenylphosphino) propane (dppp), under the same reaction conditions (−30°C) the largest known Ag cluster $[Ag_{172}Se_{40}(Se^nBu)_{92}(dppp)_4]$ is formed (Fig. 17).

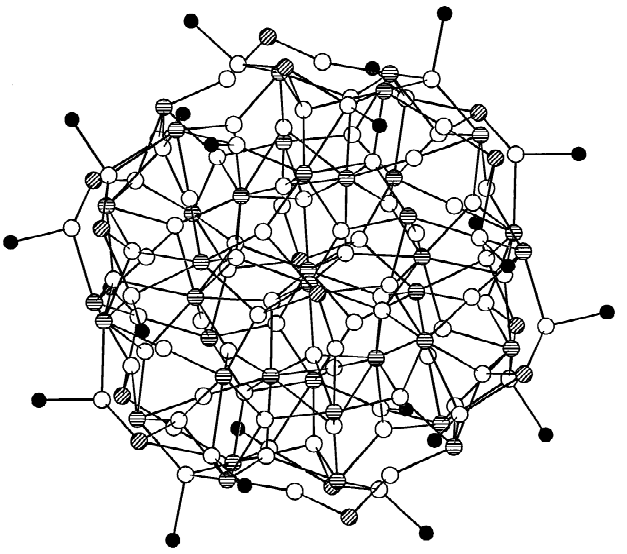

Fig. 14. Structure of $[Ag_{90}Se_{38}(Se^tBu)_{14}(PEt_3)_{22}]$ without C atoms. ○, Ag; ◍, Se^{2-}; ▨, Se atoms of the Se^{t}Bu groups; ●, P atoms.

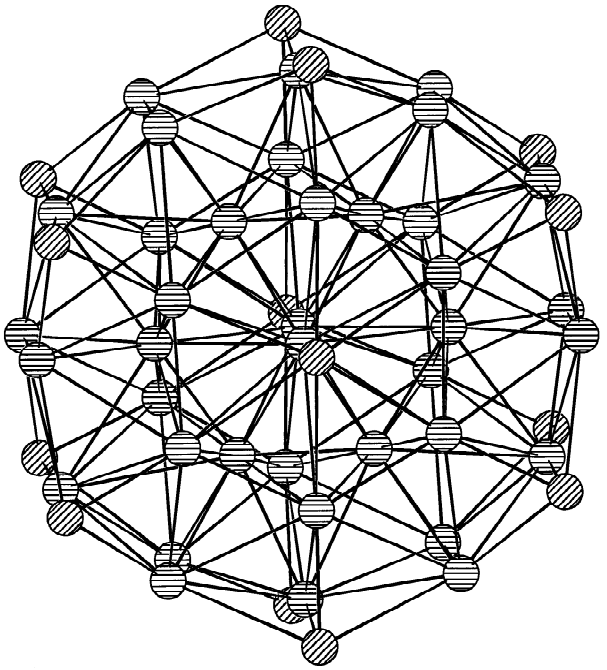

Fig. 15. Se skeleton in $[Ag_{90}Se_{38}(Se^tBu)_{14}(PEt_3)_{22}]$. ◍, Se^{2-}; ▨, Se atoms of the Se^tBu groups.

$$[Ag_{114}Se_{34}(Se^nBu)_{46}(P^tBu_3)_{14}]$$
$$\uparrow\ P^tBu_3$$
$$Ag(C_{11}H_{23}CO_2) + {}^nBuSeSiMe_3$$
$$\downarrow\ dppp$$
$$[Ag_{172}Se_{40}(Se^nBu)_{92}(dppp)_4]$$

The layer clusters of the type $\{Ag_{114}\}$ and $\{Ag_{172}\}$ are

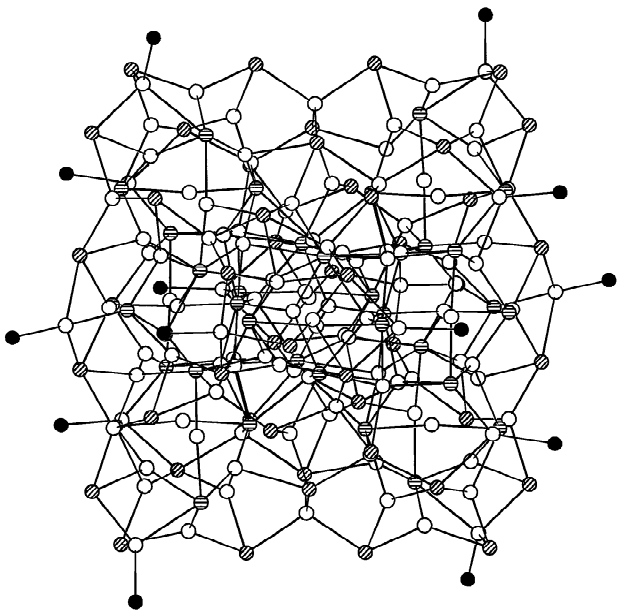

Fig. 16. Molecular structure of $[Ag_{114}Se_{34}(Se^nBu)_{46}(P^tBu_3)_{14}]$. ○, Ag; ◍, Se^{2-}; ▨, Se atoms of the Se^nBu groups; ●, P atoms of the P^tBu_3 groups.

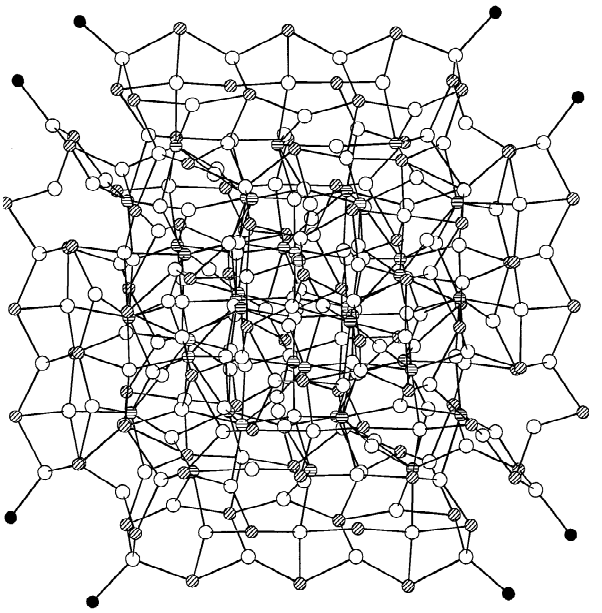

Fig. 17. Molecular structure of $[Ag_{172}Se_{40}(Se^nBu)_{92}(dppp)_4]$. ○, Ag; ◍, Se^{2-}; ▨, Se atoms of the Se^nBu groups; ●, P atoms of the dppp ligands.

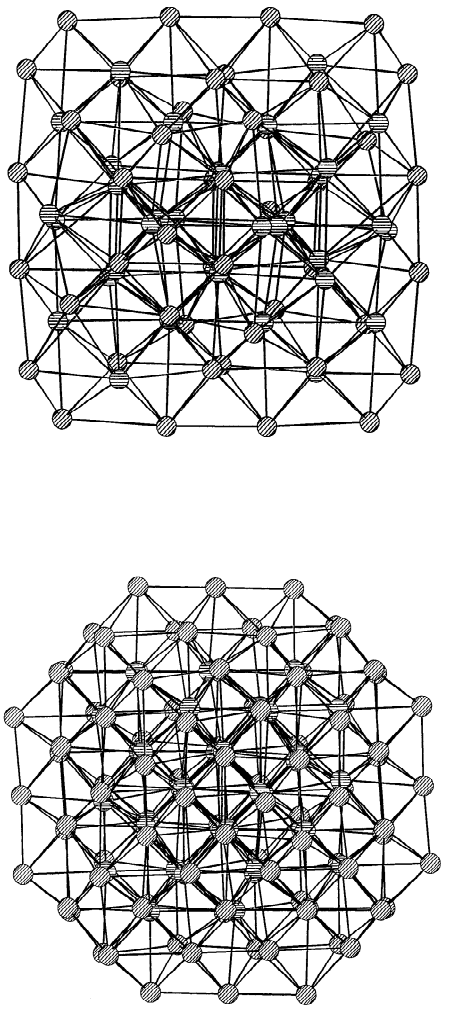

Fig. 18. Se skeleton in $[Ag_{114}Se_{34}(Se^nBu)_{46}(P^tBu_3)_{14}]$ (above) and $[Ag_{172}Se_{40}(Se^nBu)_{92}(dppp)_4]$ (below). ◍, Se^{2-}; ▨, Se atoms of the Se^nBu groups.

structurally different from the before mentioned systems, for instance from the spherical $\{Ag_{30}\}$ and $\{Ag_{90}\}$ clusters. There is a remarkable agreement between the Se skeletons in the $\{Ag_{114}\}$ and $\{Ag_{174}\}$ clusters and that of Ag_2Se [48,49] (Fig. 18). The cluster structures can realistically be described as sections of the binary phase Ag_2Se.

With increasing cluster size, the distribution of the Ag atoms in the molecular structure becomes more random. Obviously there is a tendency to a kind of disordering of the Ag atoms which is also observed in the bulk material Ag_2Se [48,49].

5. Conclusions and perspectives

It seems to be worthwhile to try to correlate aspects of nanostructured giant molecular clusters and related solid-state structures. This is valid for the molybdenum-oxide based and the coin metal–chalcogenide based systems. In order to investigate the border region between the molecular and the macroscopic world, several questions arise, for instance, whether the size of such cluster systems has a limit or whether we can fabricate ever larger assemblages approaching the limit of the macroscopic world [50,51]. Dynamic light scattering experiments for instance on solutions of the $\{Mo_{154}\}$-type clusters show the monodispersity with respect to the abundance of extremely large colloids with a hydrodynamic radius of ca. 40 nm [52], the structure of which is as yet unknown. Referring to biological systems we are dealing with a cluster size comparable to that of (spherical) viruses.

On the other hand, the nanosized polyoxomolybdate clusters now also provide model objects for studies on the initial nucleation steps of crystallization processes, an interesting aspect for solid-state chemists and physicists as the initial steps for crystal growth are not known. Recently, a novel stable ball-shaped polyoxomolybdate cluster anion with 132 Mo atoms has been synthesized [14] and seems to be particularly suited for this purpose.

References

[1] Schlenker C. Low-dimensional electronic properties of molybdenum bronzes and oxides, Kluwer, Dordrecht, 1989.

[2] Schwitzgebel G, Adams S. Electrochemical determination of small hydrogen decomposition pressures in H_xMoO_3. Ber Bunsenges Phys Chem 1988;92:1426–30.

[3] Ritter C, Müller-Warmuth W, Schöllhorn R. Structure and motion of hydrogen in molybdenum bronzes H_xMoO_3 as studied by nuclear magnetic resonance. J Chem Phys 1985;83:6130–8, and references cited therein.

[4] Atwood JL, Davies JED, MacNicol DD, Vögtle F, Lehn JM, editors. Comprehensive supramolecular chemistry, vol. 6, Solid-state supramolecular chemistry: crystal engineering and vol. 7, Solid-state supramolecular chemistry: two- and three-dimensional inorganic networks. Oxford: Pergamon/Elsevier, 1996.

[5] Voet D, Voet JG. In: 2nd ed, Biochemistry, Wiley, New York, 1995, p. 1076.

[6] Müller A, Krickemeyer E, Dillinger S, Meyer J, Bögge H, Stammler A. $[(AsOH)_3(MoO_3)_3(AsMo_9O_{33})]^{7-}$ and $[(AsOH)_6(MoO_3)_2(O_2Mo–O–MoO_2)_2(AsMo_9O_{33})_2]^{10-}$: coupling of highly negatively charged building blocks. Angew Chem Int Ed 1996;35:171–3.

[7] Pope MT, Wei X, Wassermann K, Dickman MH. New developments in the chemistry of heteropolytungstates of rhodium and cerium. Compt Rend Acad Sci Ser C 1998;297–304.

[8] Wassermann K, Dickman MH, Pope MT. Self-assembly of supramolecular polyoxometalates: the compact, water-soluble heteropolytungstate anion $[As^{III}_{12}Ce^{III}_{16}(H_2O)_{36}W_{148}O_{524}]^{76-}$. Angew Chem Int Ed 1997;36:1445–8.

[9] Müller A, Peters F, Pope MT, Gatteschi D. Polyoxometalates: very large clusters—nanoscale magnets. Chem Rev 1998;98:239–71.

[10] Pope MT, Müller A. Polyoxometalate chemistry: an old field with new dimensions in several disciplines. Angew Chem Int Ed 1991;30:34–48.

[11] Müller A, Plass W, Krickemeyer E, Dillinger S, Bögge H, Armatage A, Proust A, Beugholt C, Bergmann U. $[Mo_{57}Fe_6(NO)_6O_{174}(OH)_3(H_2O)_{24}]^{15-}$: a highly symmetrical giant cluster with an unusual cavity and the possibility of positioning paramagnetic centers on extremely large cluster surfaces. Angew Chem Int Ed 1994;33:849–51.

[12] Müller A, Krickemeyer E, Dillinger S, Bögge H, Plass W, Proust A, Dloczik L, Menke C, Meyer J, Rohlfing R. New perspectives in polyoxometalate chemistry by isolation of compounds containing very large moieties as transferable building blocks: $(NMe_4)_5[As_2Mo_8V_4AsO_{40}]\cdot 3H_2O$, $(NH_4)_{21}[H_3Mo_{57}V_6(NO)_6O_{183}(H_2O)_{18}]\cdot 65H_2O$, $(NH_2Me_2)_{18}(NH_4)_6[Mo_{57}V_6(NO)_6O_{183}(H_2O)_{18}]\cdot 14H_2O$, and $(NH_4)_{12}[Mo_{36}(NO)_4O_{108}(H_2O)_{16}]\cdot 33H_2O$. Z Anorg Allg Chem 1994;620:599–619.

[13] Huang G, Zhang S, Shao M. The remarkable polymetallate cluster: crystal structure of $Na_6[H_6Mo_{57}Fe_6O_{183}(NO)_6(H_2O)_{18}]\cdot 91H_2O$. Polyhedron 1993;12:2067–8, and references cited therein.

[14] Müller A, Krickemeyer E, Bögge H, Schmidtmann M, Peters F. Organizational forms of matter: an inorganic super fullerene and keplerate based on molybdenum oxide. Angew Chem Int Ed 1998;37:3360–3.

[15] Müller A, Krickemeyer E, Meyer J, Bögge H, Peters F, Plass W, Diemann E, Dillinger S, Nonnenbruch F, Randerath M, Menke C. $[Mo_{154}(NO)_{14}O_{420}(OH)_{28}(H_2O)_{70}]^{(25\pm5)-}$: a water-soluble big wheel with more than 700 atoms and a relative molecular mass of about 24 000. Angew Chem Int Ed 1995;34:2122–4.

[16] Müller A, Meyer J, Krickemeyer E, Diemann E. Molybdenum blue: a 200 year old mystery unveiled. Angew Chem Int Ed 1996;35:1206–8.

[17] Müller A, Krickemeyer E, Bögge H, Schmidtmann M, Beugholt C, Kögerler P, Lu C. Formation of a ring-shaped reduced 'metal oxide' with the simple composition $[(MoO_3)_{176}(H_2O)_{80}H_{32}]$. Angew Chem Int Ed 1998;37:1220–3.

[18] Müller A, Koop M, Bögge H, Schmidtmann M, Beugholt C. Exchanged ligands on the surface of a giant cluster: $[(MoO_3)_{176}(H_2O)_{63}(CH_3OH)_{17}H_n]^{(32-n)-}$. Chem Commun 1998; 1501–2.

[19] Müller A, Das SK, Fedin VP, Krickemeyer E, Beugholt C, Bögge H, Schmidtmann M, Hauptfleisch B. Rapid and simple isolation of the crystalline molybdenum-blue compounds $Na_{15}[Mo^{VI}_{126}Mo^{V}_{28}O_{462}H_{14}(H_2O)_{70}]_{0.5}[Mo^{VI}_{124}Mo^{V}_{28}O_{457}H_{14}(H_2O)_{68}]_{0.5}\cdot$ca. $400H_2O$ and $Na_{22}[Mo^{VI}_{118}Mo^{V}_{28}O_{442}H_{14}(H_2O)_{58}]\cdot$ca. $250H_2O$ with discrete and linked nanosized ring-shaped anions. Z Allg Anorg Chem, to be published.

[20] Müller A, Das SK, Bögge H, Beugholt C, Schmidtmann M. Assembling nanosized ring-shaped synthons to an anionic layer structure based on the synergetically induced complementarity of their surfaces: $Na_{21}[Mo^{VI}_{126}Mo^{V}_{28}O_{462}H_{14}(H_2O)_{54}(H_2PO_2)_7]\cdot$ca. $300H_2O$. Chem Commun, to be published.

[21] Müller A, Krickemeyer E, Bögge H, Schmidtmann M, Peters F, Menke C, Meyer J. An unusual polyoxomolybdate: giant wheels linked to chains. Angew Chem Int Ed 1997;36:484–6.
[22] Müller A, Krickemeyer E, Bögge H, Schmidtmann M, Beugholt C, Das SK, Peters F, Lu C. Giant ring-shaped building blocks linked to a layered cluster network with nanosized channels and the composition $[Mo^{VI}_{124}Mo^{V}_{28}O_{429}(\mu_3\text{-}O)_{28}H_{14}(H_2O)_{66.5}]^{16-}$. Chem Eur J, 1999;5, in press.
[23] Müller A et al., unpublished results.
[24] Müller A, Shah SQN, Bögge H, Schmidtmann M. Molecular growth from a Mo_{176} to a Mo_{248} cluster. Nature 1999;397:48–50.
[25] Ball P. Macromolecular chemistry: limits to growth. Nature 1998;395:745–8.
[26] Müller A, Hauptfleisch B, in preparation.
[27] Schmid G. Clusters and colloids. From theory to applications, VCH, Weinheim, 1994.
[28] de Jongh LJ. Physics and chemistry of metal cluster compounds, Kluwer, Dordrecht, 1994.
[29] Dance I, Fisher K. Metal chalcogenide cluster chemistry. Prog Inorg Chem 1994;41:637–803.
[30] Roof LC, Kolis JW. New developments in the coordination chemistry of inorganic selenide and telluride ligands. Chem Rev 1993;93:1037–80.
[31] Arnold J. The chemistry of metal complexes with selenolate and tellurolate ligands. Prog Inorg Chem 1995;43:353–417.
[32] Ohlmann D, Pritzkow H, Grützmacher HJ, Anthamatten M, Glaser R. A hexanuclear copper arylselenolate: synthesis, structure and proposal for its rearrangement. Chem Commun 1995;1011–2.
[33] Bonasia BJ, Mitchell GP, Hollander FJ, Arnold J. Synthesis and characterization of copper(I) and silver(I) tellurolates and selenolates. The X-ray crystal structures of $\{Cu[SeC(SiMe_3)_3]PCy_3\}_2$ and the homoleptic silver selenolate $Ag_4[SeC(SiMe_3)_3]_4$. Inorg Chem 1994;33:1797–802.
[34] Zhao J, Adcock D, Pennington WT, Kolis JW. Organotelluride chemistry: an unusual free organotelluride anion and the metal complex $[Ag_4(TeR)_6]^{2-}$ (R=thienyl). Inorg Chem 1990;29:4358–60.
[35] Dance I, Lee G. The chemistry of cadmium chalcogenide clusters $[ECd_8(E'R)_{16}]^{2-}$, $[E_4Cd_{10}(E'R)_{16}]^{4-}$, and $[E_4Cd_{17}(E'R)_{28}]^{2-}$. Spec Publ R Soc Chem 1993;131:87–94.
[36] Brennan JG, Siegrist T, Carroll PJ, Stuczynski SM, Reynders P, Brus LE, Steigerwald ML. Bulk and nanostructure group II–VI compounds from molecular organometallic precursors. Chem Mater 1990;2:403–9.
[37] Fenske D, Ohmer J, Hachgenei J. New Co and Ni clusters with Se and PPh_3 as ligands: $[Co_4(\mu_3\text{-}Se)_4(PPh_3)_4]$, $[Co_6(\mu_3\text{-}Se)_8(PPh_3)_6]$, $[Co_9(\mu_4\text{-}Se)_3(\mu_3\text{-}Se)_8(PPh_3)_6]$ and $[Ni_{34}(\mu_5\text{-}Se)_2(\mu_4\text{-}Se)_{20}(PPh_3)_{10}]$. Angew Chem Int Ed 1985;24:993–5.
[38] Fenske D, Ohmer J, Hachgenei J, Merzweiler K. New transition metal clusters with ligands from main groups five and six. Angew Chem Int Ed 1988;27:1277–96.
[39] Krautscheid H, Fenske D, Baum G, Semmelmann M. A new copper selenide cluster with PPh_3 ligands: $[Cu_{146}Se_{73}(PPh_3)_{30}]$. Angew Chem Int Ed 1993;32:1303–5.
[40] Fenske D, Krautscheid H. Synthesis and structure of novel Cu clusters: $[Cu_{30-x}Se_{15}(PiPr_3)_{12}]$ ($x=0,1$) and $[Cu_{36}Se_{18}(PtBu_3)_{12}]$. Angew Chem Int Ed 1990;29:796–9.
[41] Dehnen S, Schäfer A, Ahlrichs R, Fenske D. An ab initio study of structures and energetics of copper sulfide clusters. Chem Eur J 1996;2:429–35.
[42] Dehnen S, Schäfer A, Fenske D, Ahlrichs R. New sulfur- and selenium-bridged copper clusters: ab initio calculations on $[Cu_{2n}Se_n(PH_3)_m]$ clusters. Angew Chem Int Ed 1994;33:746–8.
[43] van der Putten D, Olevano D, Zanoni R, Krautscheid H, Fenske D. Photoemission from large-nuclearity copper selenide clusters. J Electron Spectrosc 1995;76:207–11.
[44] Corrigan JF, Fenske D. Butyltellurolate ligands in cluster synthesis: molecular structures of Ag_6Te_6, $Ag_{32}Te_{25}$ and $Ag_{48}Te_{36}$ complexes. J Chem Soc 1996;943–4.
[45] Corrigan JF, Fenske D. Mono- and bis-silylated tellurium reagents in silver-telluride cluster synthesis: characterisation of $Ag_{30}Te_{21}$ and $Ag_{46}Te_{29}$ complexes. Chem Commun 1997;1837–8.
[46] Corrigan JF, Fenske D, Power WP. Silver-tellurolate polynuclear complexes: from isolated cluster units to extended polymer chains. Angew Chem Int Ed 1997;36:1176–8.
[47] Fenske D, Zhu N, Langetepe T. Synthesis and structures of new Ag–Se clusters: $[Ag_{30}Se_8(SetBu)_{14}(PnPr_3)_8]$, $[Ag_{90}Se_{38}(SetBu)_{14}(PEt_3)_{22}]$,$[Ag_{114}Se_{34}(SenBu)_{46}(PtBu_3)_{14}]$, $[Ag_{112}Se_{32}(SenBu)_{48}(PtBu_3)_{12}]$, and $[Ag_{172}Se_{40}(SenBu)_{92}(dppp)_4]$. Angew Chem Int Ed 1998;37:2640–4.
[48] Wiegers GA. The crystal structure of the low-temperature form of silver selenide. Am Mineral 1971;56:1882–8.
[49] Pinsker ZG, Chiangliang C, Imamov RM, Lapidus EL. Determination of the crystal structure of the low-temperature phase α-Ag_2Se. Sov Phys Crystallogr (Engl Tansl) 1965;7:225–31.
[50] Müller A. Supramolecular inorganic species: an expedition into a fascinating, rather unknown land mesoscopia with interdisciplinary expectations and discoveries. J Mol Struct 1994;325:13–35.
[51] Müller A, Pope MT. Increasing the size of polyoxometalates: emergent properties upon self-assembly and condensation processes. In: Mainzer K, Müller A, Saltzer WG, editors. From simplicity to complexity, part II, information—interaction—emergence, Vieweg, Wiesbaden, 1998;57–68.
[52] Müller A, Eimer W, Diemann E, Serain C. To be published.